

## LHCb measurements on CPV in $B$ decays ( $B \rightarrow 3h$ , $\phi_s$ , charmless $B$ decays)

---

**Ekaterina Govorkova\***

*Nikhef National institute for subatomic physics*

*E-mail: [ekaterina.govorkova@cern.ch](mailto:ekaterina.govorkova@cern.ch)*

The latest results on the  $CP$  violation measurements in  $B$  decays are reported. The measurement of the weak phase  $\phi_s^{s\bar{s}}$  using the  $B_s^0 \rightarrow \phi\phi$  decay mode is performed on a dataset corresponding to an integrated luminosity of  $5 fb^{-1}$  collected in proton-proton collisions by the LHCb experiment. Results on the first ever measurement of the  $CP$ -violating phase  $\phi_s^{d\bar{d}}$  using  $B_s^0 \rightarrow (K^+\pi^-)(K^-\pi^+)$  channel, based on  $3 fb^{-1}$  of data, are summarised.

*Sixth Annual Conference on Large Hadron Collider Physics (LHCP2018)*

*4-9 June 2018*

*Bologna, Italy*

---

\*Speaker.

## 1. CP violation and the LHCb detector

There are three types of CP violation (CPV) that can occur in the  $B$  meson system. One of them is CPV in decay, it takes place when the probability of a  $B$  meson to decay to its final state is not equal to the probability of its antiparticle to decay to the CP-conjugate final states. This type of CP violation is the only type that is allowed for charged  $B$  mesons. Neutral  $B$  mesons can oscillate and undergo transition to the  $\bar{B}$  meson and vice-versa. However, if the probability of a  $B$  meson transiting to a  $\bar{B}$  meson is not the same as the opposite process, then CP violation occurs in mixing. The third type of CPV occurs in the interference between direct decay and when  $B$  meson first oscillates and then decays. It is specific for neutral  $B$  mesons decays to the non flavour-specific final states.

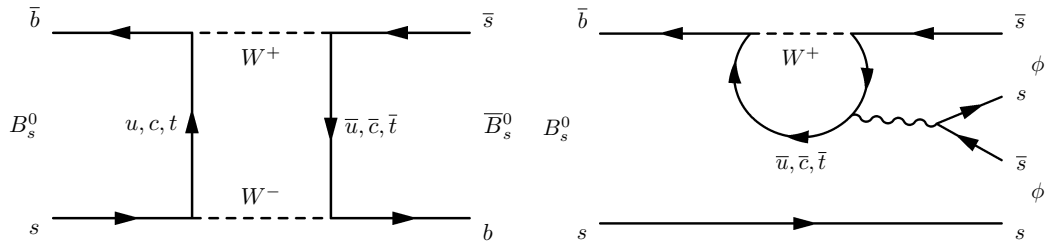


**Figure 1:** Feynman diagram (left) of  $B_s^0$  mixing and (right) of  $B_s^0 \rightarrow \phi\phi$  decay.

The ability to perform time-dependent analysis implies several constraints on the detector design and performance. Out of the four main experiments situated at the Large Hadron Collider (LHC) at CERN, the LHCb detector [1] is the one that is dedicated to study  $b$ - and  $c$ - hadrons, especially to the CP violation measurements. One of the key ingredients to time-dependent measurements is the decay-time resolution, since it is crucial to be able to resolve  $B$  meson oscillations, the  $B_s^0$  meson oscillation frequency is around  $18 \text{ ps}^{-1}$ . The VELO sub-detector of LHCb allows for the extremely precise measurement of the decay-length, with resolution of approximately 45 fs [2].

In order to measure time-dependent decay rate it is necessary to know the flavour of a  $B$  meson at production. Several flavour-tagging (FT) algorithms are used at LHCb that provide the estimated tag of  $B$  meson at production together with the probability of an incorrect tag. There are two classifications of FT algorithms, the first kind is called same-side and uses information from particles associated to the signal  $B$  meson fragmentation. Second type is referred to as opposite-side algorithms, which use the fact that  $b$  and  $\bar{b}$  quarks are produced in pairs and infer the flavour of the signal  $B$  meson from flavour-specific decays of the opposite  $B$  meson.

## 2. Measurement of $\phi_s^{s\bar{s}}$ using $B_s^0 \rightarrow \phi\phi$

The  $\phi_s^{s\bar{s}}$  phase arises in the interference between the amplitudes of a  $B_s^0$  meson decaying via  $b \rightarrow s\bar{s}s$  transition directly to its final state or after oscillation to a  $\bar{B}_s^0$  meson. The value of  $\phi_s^{s\bar{s}}$  is small in the Standard Model: the upper limit is predicted to be 0.02 rad based on calculations using quantum chromodynamics factorisation [3]. The measurement is based on data collected in 2011, 2012, 2015 and 2016 by the LHCb detector, which corresponds to an integrated luminosity of approximately  $5 \text{ fb}^{-1}$ .

In order to select signal  $B_s^0 \rightarrow \phi(\rightarrow K^+K^-)\phi(\rightarrow K^+K^-)$  candidates from background candidates, a multilayer perceptron (MLP) is used [4]. Simulated signal candidates are used as a proxy for signal and the four-kaon invariant-mass sidebands from data are used as a background proxy in the training of an MLP. Cut-based vetoes are applied in order to reduce the contribution from  $B^0 \rightarrow \phi K^*$  peaking background, when one of the pions in the final state is identified as a kaon. Another peaking contribution comes from  $\Lambda_b \rightarrow \phi p K$  and due to its broad shape directly in the signal region it is taken into account in the mass fit instead of being vetoed. The mass fits to the four-kaon invariant mass are shown in Fig. 2, where approximately 8500  $B_s^0$  candidates are found. The  $s$ Plot procedure is used in order to subtract the remaining background contributions and to perform further analysis only on the weighted signal  $B_s^0$  candidates.

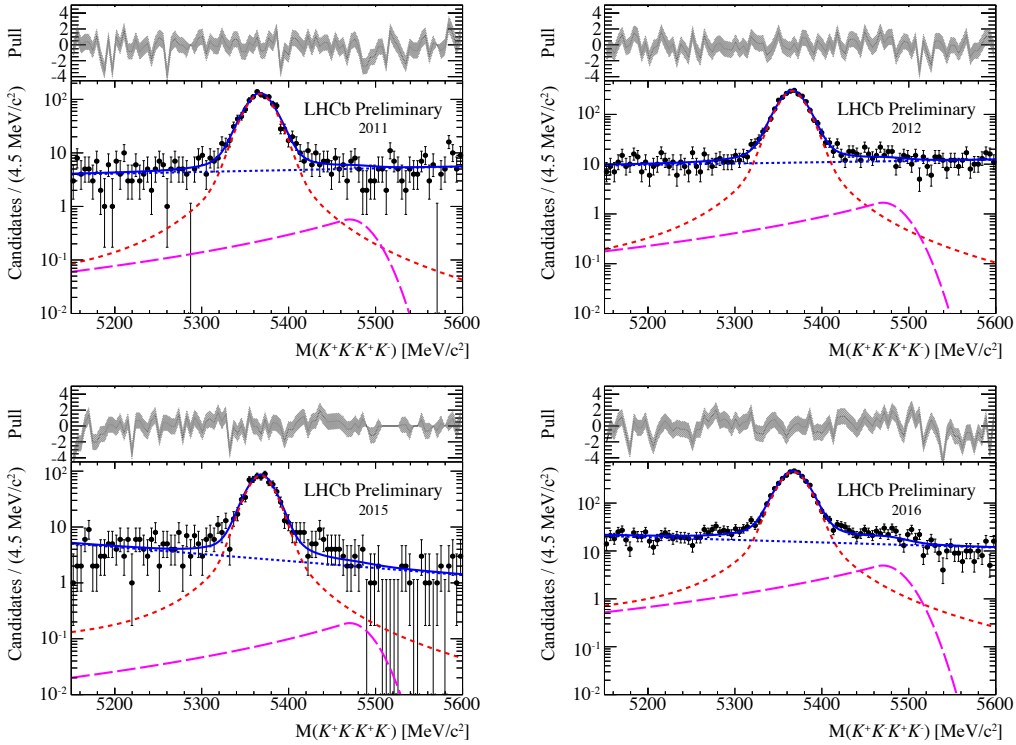


**Figure 2:** A fit to the 2011 (top left), 2012 (top right), 2015 (bottom left) and 2016 (bottom right) data which is represented by the black points. The results of the total fit are shown (blue solid line), with the  $B_s^0 \rightarrow \phi\phi$  (red dashed), the  $\Lambda_b \rightarrow \phi p K^-$  (magenta long dashed), and the combinatorial (blue short dashed) fit components.

An angular analysis is performed on the signal  $B_s^0 \rightarrow \phi\phi$  candidates in order to disentangle CP eigenstates. The angles are defined in the helicity basis, shown in Fig. 3. The  $B_s^0 \rightarrow \phi\phi$  decay is a decay of a pseudoscalar to two vector mesons. However, there are contributions of  $S$ -wave and double  $S$ -wave processes as well, where  $S$  denotes the contribution from a non-resonant pair of kaons or a spin-0 meson contribution, i.e. an  $f_0(980)$  meson. The total amplitude is a coherent sum of  $P$ -,  $S$ - and double  $S$ -wave processes and is modelled using the different functions of the helicity angles associated with these terms. Four observables, the decay time and the three helicity angles, are used to fully describe the  $B_s^0 \rightarrow \phi\phi$  system.

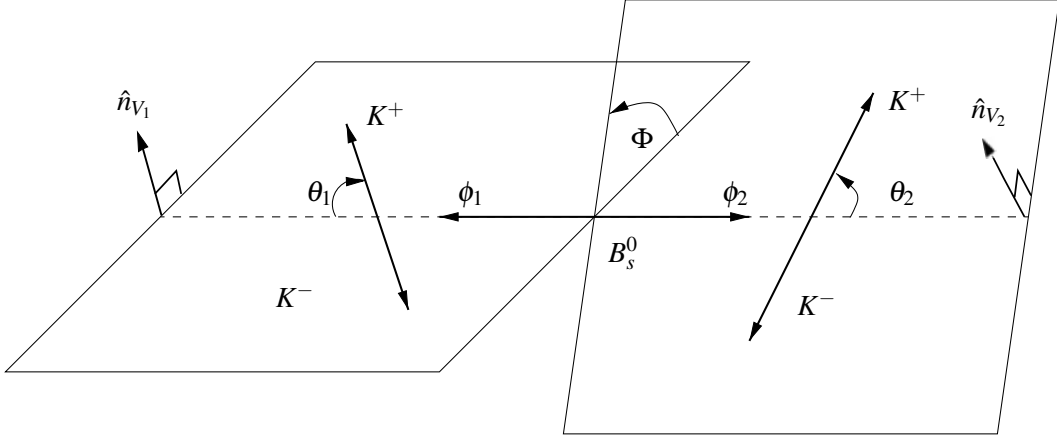


**Figure 3:** Decay angles for the  $B_s^0 \rightarrow \phi\phi$  decay, where  $\theta_{1,2}$  is the angle between the  $K^+$  track momentum in the  $\phi_{1,2}$  meson rest frame and the parent  $\phi_{1,2}$  momentum in the  $B_s^0$  rest frame,  $\Phi$  is the angle between the two  $\phi$  meson decay planes and  $\hat{n}_{V_{1,2}}$  is the unit vector normal to the decay plane of the  $\phi_{1,2}$  meson.

Several experimental effects should be taken into account when performing the measurement. All time-dependent terms are convolved with a Gaussian function with the width estimated separately for each candidate based on the uncertainty obtained from the vertex and kinematic fit, to account for the effect of the decay time resolution. The calibration of the per-event decay-time uncertainty is performed using samples of prompt data, which consists of the tracks that originate from the primary interaction vertex. Another effect is selection efficiency. Selection criteria used in the trigger suppress the background originating from the primary vertex, but introduce a decay-time dependent acceptance. The efficiency is taken from the  $B_s^0 \rightarrow D_s^- (\rightarrow K^+ K^- \pi^-) \pi^+$  decay, in the case of data taken in 2011 and 2012, and from the  $B_d^0 \rightarrow J/\psi (\rightarrow \mu^+ \mu^-) K^* (\rightarrow K^+ \pi^-)$  decay in the case of data taken in 2015 and 2016. The reason for different calibration channels is due to changes in the selection used in the trigger between different data-taking periods. Cubic splines are used to construct the acceptance as a function of decay time in the probability density function (PDF). Due to the geometry of the LHCb detector and the momentum requirements imposed on the final-state particles, the efficiency as a function of the helicity angles is also not flat. The angular efficiency is parametrised in the same basis as the angular functions and is calculated by means of the Monte Carlo integration. As described in the previous section, there are two types of FT algorithms used in LHCb, both types are used to tag the flavour of the  $B_s^0$  at production. The performance of the algorithms is calibrated using control modes, the details of the calibration procedure are described in Ref. [5].

Accounting for the acceptance and resolution effects in the PDF, parameter estimation is achieved using minimization of the negative log-likelihood and  $\phi_s^{s\bar{s}}$  is measured to be  $-0.07 \pm 0.13$  (stat)  $\pm 0.03$  (syst) rad. The distributions of the  $B_s^0$  decay time and three helicity angles together with the projections of the fit result are shown in Fig. 4.

### 3. Measurement of $\phi_s^{d\bar{d}}$ using $B_s^0 \rightarrow (K^+ \pi^-)(K^- \pi^+)$

The measurement of the mixing-induced  $CP$ -violating phase,  $\phi_s^{d\bar{d}}$ , in  $b \rightarrow d\bar{d}s$  transitions is performed, using  $B_s^0 \rightarrow (K^+ \pi^-)(K^- \pi^+)$  decay. This is the first measurement of  $\phi_s^{d\bar{d}}$  ever per-

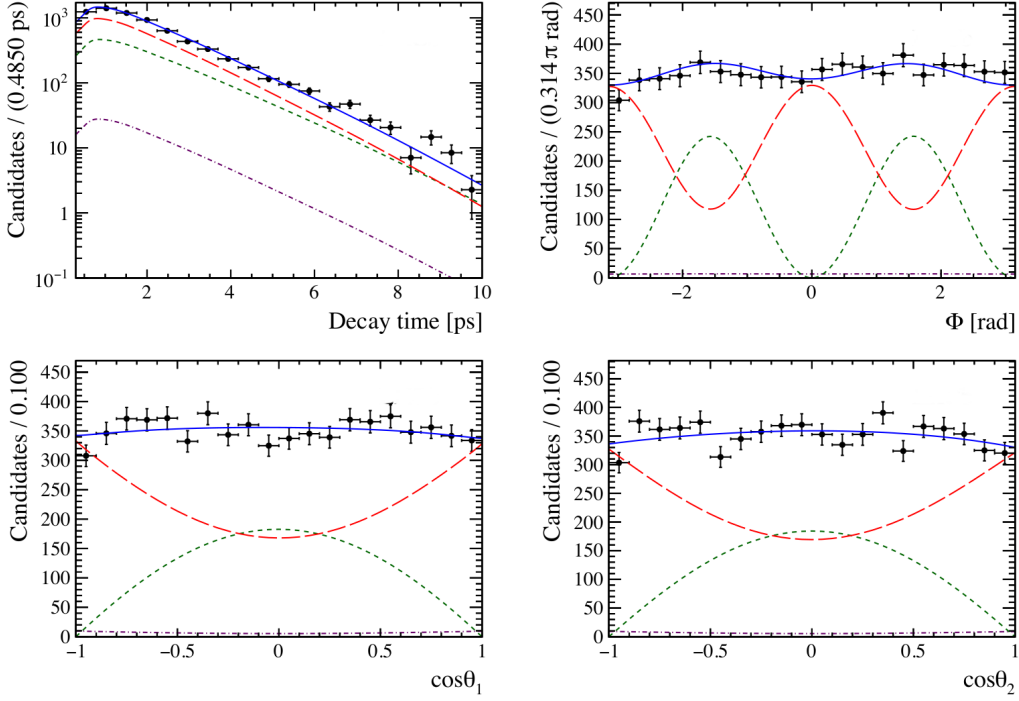


**Figure 4:** One-dimensional projections of the  $B_s^0 \rightarrow \phi\phi$  fit for (top-left) decay time with binned acceptance, (top-right) helicity angle  $\Phi$  and (bottom-left and bottom-right) cosine of the helicity angles  $\theta_1$  and  $\theta_2$ . The background-subtracted data are marked as black points, while the blue solid lines represent the projections of the best fit. The CP-even  $P$ -wave, the CP-odd  $P$ -wave and  $S$ -wave combined with double  $S$ -wave components are shown by the red long dashed, green short dashed and purple dot-dashed lines, respectively. Fitted components are plotted taking in to account efficiencies in the time and angular observables.

formed. The flavour-tagged time-dependent angular analysis of the  $B_s^0 \rightarrow (K^+\pi^-)(K^-\pi^+)$  is similar to the  $B_s^0 \rightarrow \phi\phi$  decay described in the previous section, therefore only specific steps that are not present in  $\phi_s^{s\bar{s}}$  are described in the following. The measurement of  $\phi_s^{d\bar{d}}$  is based on the datasets collected in 2011 and 2012 by the LHCb detector and correspond to an integrated luminosity of  $3 \text{ fb}^{-1}$ .

The  $K\pi$  mass spectrum in the range  $750\text{-}1600 \text{ MeV}/c^2$  is studied, which is dominated by  $K_0^*(800)^0$ ,  $K_0^*(1430)^0$ ,  $K^*(892)^0$  and  $K_2^*(1430)^0$  resonances that are scalar, vector and tensor contributions, respectively. One single amplitude in modes involving  $K\pi$  pair, three amplitudes for vector-vector or vector-tensor decays and five amplitudes for a tensor-tensor decay are allowed according to angular momentum conservation. The signal  $B_s^0 \rightarrow (K^+\pi^-)(K^-\pi^+)$  candidates are selected in a similar manner to the  $B_s^0 \rightarrow \phi\phi$  decay, but the signal region contains more peaking background contributions. The mass fit together with all the background contributions are shown in Fig. 5. The corresponding fit finds approximately 6000 signal  $B_s^0 \rightarrow (K^+\pi^-)(K^-\pi^+)$  candidates. Accounting for the acceptance and resolution effects, the value of  $\phi_s^{d\bar{d}}$  is found to be  $-0.10 \pm 0.13 \text{ (stat)} \pm 0.14 \text{ (syst)}$  rad, which is in agreement with the hypothesis of  $CP$  conservation.

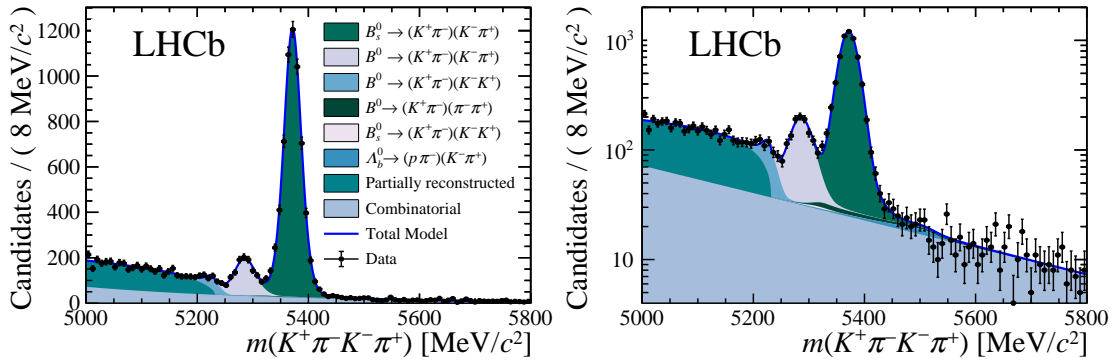


**Figure 5:** Four-body invariant mass distribution on a (left) linear and (right) logarithmic scale superimposed with the mass fit model.

#### 4. Summary and outlook

This document describes two flavour-tagged time-dependent angular analyses based on data collected by the LHCb experiment. The weak phases  $\phi_s^{s\bar{s}}$  and  $\phi_s^{d\bar{d}}$  are both found to be consistent with zero in the current statistical precision. Enlarged data samples are required to increase the statistical precision and determine the presence of the  $CP$  violation in this decay modes. The measured and extrapolated statistical sensitivities for  $CP$  violating phases are shown in Fig. 6. For  $\phi_s^{s\bar{s}}$  a statistical uncertainty of 0.011 rad can be achieved with  $300 \text{ fb}^{-1}$  of data collected after an upgrade of the LHCb detector. Many systematic uncertainties are measured using control channels and therefore are expected to scale with integrated luminosity. The measurement of  $\phi_s^{s\bar{s}}$  is expected to be statistically limited even with data, collected after the upgrade. In the current  $\phi_s^{d\bar{d}}$  analysis the same weak phase is assumed for all contributions. With increased statistical precision, it will be possible to determine the phase separately for each contribution and check possible polarisation dependence in the  $B_s^0 \rightarrow K^*(892)^0 \bar{K}^*(892)^0$  decay.

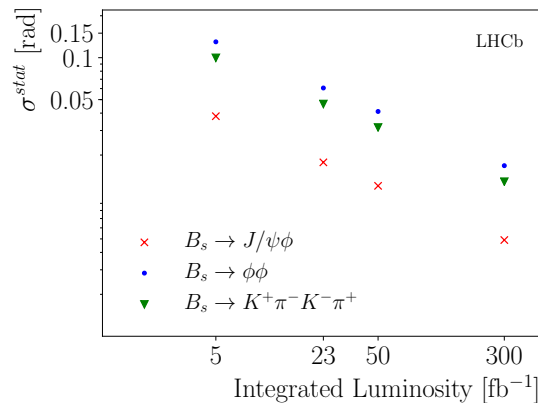


**Figure 6:** Comparison of  $\phi_s$  sensitivity from different decay modes.

## References

- [1] LHCb collaboration, A. A. Alves Jr. et al., *The LHCb detector at the LHC*, JINST **3** (2008) S08005.
- [2] LHCb collaboration, R. Aaij et al., *LHCb detector performance*, Int. J. Mod. Phys. **A30** (2015) 1530022, arXiv:1412.6352.
- [3] H.-Y. Cheng, C.-K. Chua, *QCD factorization for charmless hadronic  $B_s$  decays revisited*, Phys. Rev. **D80** (2009) 114026.
- [4] L. Breiman, J. H. Friedman, R. A. Olshen, C. J. Stone, *Classification and regression trees*, Wadsworth international group, Belmont, California, USA 1984.
- [5] LHCb collaboration, R. Aaij et al., *Precision measurement of CP violation in  $B_s^0 \rightarrow J/\psi K^+ K^-$  decays*, Phys. Rev. Lett. **114** (2015) 041801, arXiv:1411.3104.